Dynamic analysis of a DP-FPSO: offloading with DP and non-DP shuttle tankers in the Gulf of Mexico

Eduardo A. Tannuri[1], Celso P. Pesce[2], Alexandre N. Simos[3], Carlos H. Fucatu[3], Paulo R. Ferreira[4], Nicholas Howard[5]

Escola Politécnica, University of São Paulo
(1) Mechatronics Engineering Department
(2) Mechanical Engineering Department, Fluid-Structure Interaction and Offshore Mechanics Laboratory
(3) Naval Architecture and Ocean Engineering Department, Numerical Offshore Tank

(4) PETROBRAS America*
(5) Chevron Shipping Co. - Marine Services Group

Abstract

The present paper addresses a comprehensive analysis carried out with a DP-FPSO (Dynamic Positioned-FPSO) for the Gulf of Mexico (GoM). As an outcome of this, a methodology for evaluating the DP-FPSO response and its offloading alternatives was devised, including different failure possibilities. Fully time-domain dynamic simulations were carried out in order to analyze the DP-FPSO stationkeeping ability under different environmental conditions, to determine drifting times after a blackout and to analyze the behavior of the vessel in drive-off situations. Simulations also allowed determining limit environmental conditions for offloading operations, considering either a non-DP or a DP Shuttle Tanker (ST), restrained within the boundaries of the allowable excursion that is dictated by the riser/flexible jumper design.

Keywords

Dynamic Positioning, FPSO, riser, simulation

1 Introduction[1]

The recent and catastrophic events occurred in the Gulf of Mexico, the 2005 Atlantic hurricane season[2] , pushed the offshore oil industry towards new concepts of production platforms. The Hurricane Katrina, one of the most intense, is depicted in Figure 1. A promising alternative, regarding safety, is the DP-FPSO (Dynamic Positioned-FPSO). In this concept, risers are installed to the FPSO unit by means of a disconnectable turret, allowing the vessel to weathervane freely and to be disconnected under harsh conditions. Nonetheless, though ideally simple, such a concept must be confronted with usual ones through a robust technical analysis concerning not only the ability of keeping position in usual operational conditions but, primarily, the consequences of possible failures, as black-outs or driving-offs. Though not common, such failure events are rather probable (Chen and Moan, 2004).

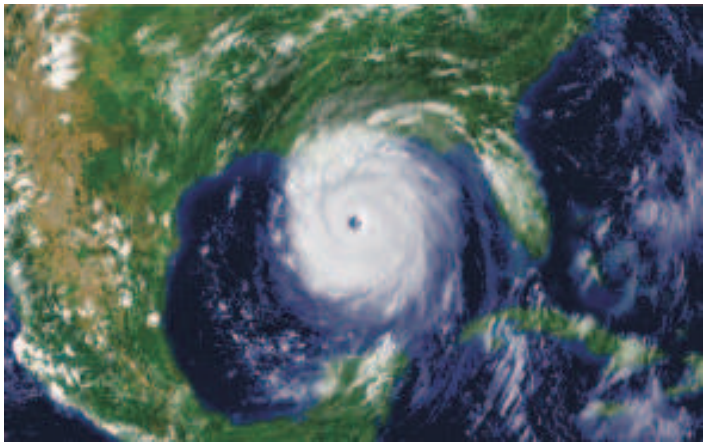

Fig. 1 NOOA Satellite Image of Hurricane Katrina taken on August, 28th, 2005. Source: NOOA (http://hurricanes.noaa.gov/)

1 A shortened and first version of this paper was presented at the 3rd IWAOH - 3rd International Workshop on Applied Offshore Hydrodynamics, RJ, 2007.

2 According to NOAA, (http://hurricanes.noaa.gov/): "The 2005 Atlantic hurricane season is the busiest on record and extends the active hurricane cycle that began in 1995 - a trend likely to continue for years to come. The season included 28 named storms, including 15 hurricanes in which seven were major (Category 3 or higher)".

* Formerly with Chevron

To face this complex technical problem, a thorough and comprehensive analysis program was planned by Chevron, Devon, Statoil and other partners aiming at dimensioning DP and turret disconnection systems for a FPSO and a ST (Shuttle Tanker) to operate in the Gulf of Mexico (GoM). This analysis encompassed: DP capability study of both: the FPSO and the DP-ST; offloading alternatives (bow loading / side loading; ship to ship transfer); taut / slack hawser study; floating hose study; project looking back at similar conversions; Jones Act Tanker[2] availability study. A typical offloading operation is illustrated in Figure 2.

The system should meet the following general design premises:

- DP-FPSO removable in a Hurricane;
- on station more than 95% of time;
- DP capable of long term operations without downtime;
- offloading to shuttle tanker in tandem;
- DP or a non-DP ST.

Fig. 2 Typical Offloading Operation.

One of the major issues, the DP capability study, concerned the non-linear dynamic analysis of the system under the action of waves, current and wind. The present paper addresses such analysis, carried out with a DP-FPSO. Time-domain dynamic simulations were carried out, in order to address the DP-FPSO station keeping ability under operational environmental conditions, to determine drifting times after a blackout and to address the behavior of the vessel in drive-off situations. Simulations also allowed determining maximum environmental conditions for the offloading operations, considering either a non-DP or a DP Shuttle Tanker (ST) the allowable excursion dictated by the riser/flexible jumper design.

All cases were run with a full non-linear time-domain simulation code, which takes into account wave drift (Aranha, 1994; Aranha and Martins, 2001; Aranha et al., 2001), current loads (Simos et al., 2001) and wind forces (OCIMF, 1994). The simulation code also comprises: extended Kalman filtering with PD controller[3]; wind feed-forward compensation algorithm; optimal thrust allocation algorithm with shadow zone constraints; azimuthal-thruster dynamics; hawser, mooring and risers dynamics; providing the following main outputs: time-histories of all signals such as positioning and respective errors, thrust forces, delivered power and hawser tension, besides their main statistic parameters. A full description of DP features included in the simulation code is presented in Bravin and Tannuri (2004) and Tannuri (2002). Two different goals are pursued in this article. First of all, considering the original aspects of the new FPSO concept, the paper aims to outline the methodology and the different set of criteria adopted in this study. Additionally, the second purpose is to present and discuss the most important results, indicating limiting factors and critical operational aspects derived from the analysis.

Before discussing the analysis itself, however, a brief description of the time-domain simulation code is presented, in order to highlight the main features included in the dynamic analysis and how they are modeled. Details on the theoretical models, especially regarding the control algorithms, are presented in the Appendix.

2 The offshore system simulator

A time domain numerical procedure designed for the analysis of moored and DP offshore systems was used. The inputs of the simulator are:

- Floating body main parameters (dimensions, mass matrix, etc.);
- Aerodynamic drag coefficients (following standard given by OCIMF, 1994);
- Current coefficients (following standard given by OCIMF, 1994) or hydrodynamic derivatives;
- Hydrodynamic coefficients (potential damping, added mass, first and second order wave force coefficients);
- Environmental conditions (wave and wind spectra, current); Mooring and risers system characteristics;
- Thrusters characteristics and layout;
- DP modes and parameters.

The non-linear time-domain simulation runs in a parallel processing computer cluster and outputs time series describing the motions of the floating unities (FU) in six degrees of freedom (6dof), tensions on the mooring lines and hawser, propellers thrust and power, etc., and a corresponding statistical summary. 3D-stereo visualization outputs are also available.

2.1 Ship dynamics and environmental action modeling

For the purpose of evaluating the DP system, only the horizontal motions of the ship must be considered and the mathematical model can be built by applying mechanical laws. The low-frequency motion of the system can be conveniently

2 Vessels satisfying the requirements given by the US Merchant Marine Act of 1920, often called The "Jones Act".
3 Though not usual, other alternative controlling algorithms are also implemented, e.g., slide-mode (Tannuri, Donha and Pesce, 2001), or adaptive techniques (Tannuri, Kubota and Pesce, 2006).

expressed in two orthogonal reference systems, one being the Earth-fixed ($OXYZ$) and the other ($Gx_1x_2x_3$) a non-inertial reference frame fixed on the vessel (see Figure 3). The origin of this reference frame is the intersection of the midship section with the longitudinal plane of symmetry of the ship, and it is taken as the center of gravity (G). Additionally, the axes of reference frame are taken to be coincident with the principal axes of inertia of the vessel. Bearing in mind these assumptions, the resulting equations of low-frequency motions are:

$$\begin{aligned}
&(M+M_{11})\ddot{x}_{1L}-(M+M_{22})\dot{x}_{2L}\dot{x}_{6L}-M_{26}\dot{x}_{6L}^{\,2}+C_{11}\dot{x}_{1L}=F_{1E}+F_{1T}+F_{1M}\\
&(M+M_{22})\ddot{x}_{2L}+M_{26}\ddot{x}_{6L}+(M+M_{11})\dot{x}_{1L}\dot{x}_{6L}+C_{22}\dot{x}_{2L}=F_{2E}+F_{2T}+F_{2M}\\
&(I_Z+M_{66})\ddot{x}_{6L}+M_{26}\ddot{x}_{2L}+M_{26}\dot{x}_{1L}\dot{x}_{6L}+C_{66}\dot{x}_{6L}=F_{6E}+F_{6T}+F_{6M}
\end{aligned} \tag{1}$$

where I_z is the moment of inertia about the vertical axis; M is the mass of the vessel, C_{ij} are damping coefficients, M_{ij} are added mass terms, F_{1E}, F_{2E}, F_{6E} are surge, sway and yaw environmental loads (current, wind and waves), F_{1T}, F_{2T}, F_{6T} are forces and moment delivered by the propulsion system and F_{1M}, F_{2M}, F_{6M} are forces and moment due to risers, mooring lines and hawser, if any. The variables $\dot{x}_{1L}$ and $\dot{x}_{2L}$ are surge and sway low-frequency velocities and $\dot{x}_{6L}$ is the yaw rate.

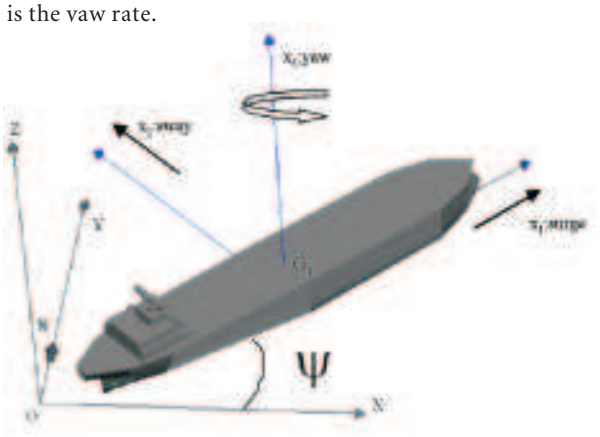

Fig. 3 Coordinate systems

The position and heading of the vessel related to the Earth-fixed coordinate system are obtained from the following equation:

$$\begin{pmatrix}\dot{X}_L\\ \dot{Y}_L\\ \dot{\psi}_L\end{pmatrix}=\mathbf{T}(\psi)\begin{pmatrix}\dot{x}_{1L}\\ \dot{x}_{2L}\\ \dot{x}_{6L}\end{pmatrix},\ \text{with}\ \mathbf{T}(\psi_L)=\begin{pmatrix}\cos(\psi_L) & -\sin(\psi_L) & 0\\ \sin(\psi_L) & \cos(\psi_L) & 0\\ 0 & 0 & 1\end{pmatrix} \tag{2}$$

Wave-frequency (first-order) motions X_H, Y_H, ψ_H are evaluated by means of transfer functions related to the wave height, namely, the so-called Response Amplitude Operators (RAOs), and are obtained via numerical methods modeling the potential flow around the hull. Such an approach is grounded on the assumption of linear response of wave-frequency motions and on the uncoupling between wave-frequency and low-frequency motions. Therefore, the real position of the vessel X, Y, ψ can be given by:

$$\begin{pmatrix}X\\ Y\\ \psi\end{pmatrix}=\begin{pmatrix}X_L\\ Y_L\\ \psi_L\end{pmatrix}+\begin{pmatrix}\dot{X}_H\\ \dot{Y}_H\\ \dot{\psi}_H\end{pmatrix} \tag{3}$$

Current forces and moments may be evaluated through four distinct models: (i) OCIMF Model (OCIMF, 1994); (ii) a cross-flow model; (iii) a hydrodynamic derivatives maneuvering model; (iv) an Heuristic Model, (Simos et al., 2001; Tannuri et al., 2001). All models include the possibility of considering constant or time varying current profiles.

The simulator covers both cases: constant or gust wind. In the latter case, wind spectra are the usual Harris, Wills and API types.

Wave action can be regular and irregular. For irregular waves the following common unidirectional spectra are implemented: Pierson-Moskowitz, JONSWAP and Gaussian. First and second-order wave effects are modeled and wave-drift damping effects are included, according to Aranha (1994) and Aranha and Martins (2001). Both, first and second order hydrodynamic coefficients in waves are determined by running WAMIT® code (2000).

2.2 DP algorithms and propeller model

Usually, three main classes of algorithms are used in commercial DP systems. A low-pass filter, called wave-filter, separates wave-frequency components from the measured signals. Such decomposition is mandatory, as the DP system is able to control only low-frequency motions. High-frequency motion control would require an enormous power and could cause extra tear and wear in propellers. Normally, an Extended Kalman Filter is used to perform such a task.

Furthermore, a thrust allocation algorithm has to be used to distribute control forces to the thruster system. This algorithm guarantees minimum power consumption, generating the required total forces and moment to keep the vessel position. At last, a control algorithm uses filtered motion measurements to calculate such required thrusts. Commercial DP Systems use a Proportional-Derivative (PD) controller, coupled to a wind feed-forward term. Such a term enables one to estimate the wind load action on the vessel (based on wind sensor measurements), thus compensating it by means of the action of propellers. The formulation of the Extended Kalman filter, thrust allocation algorithm and controller adopted in the simulations is presented in the Appendix.

The simulator includes models for controllable pitch propellers (cpp) and for fixed pitch propellers (fpp). The model takes into account their characteristic curves, and is able to estimate real power consumption and delivered thrust. For fpp propellers, dynamics of rotating parts are also simulated, accounting for the delay between the control command and the propeller response due to the inertia of the system. Furthermore, for cpp propellers, a maximum pitch variation rate is defined in order to simulate the governing mechanism that is responsible for the pitch variation.

3 Analysis of FPSO/ST for the gulf of Mexico

A complete simulation analysis was for a disconnectable DP-FPSO designed as an option for operating in the GoM, considering two offloading options: DP or non-DP ST. FPSO is based on the MV Aberdeen, a 560,000bbls tanker. The turret is installed in a lateral-forward position, as indicated in Figure 4.

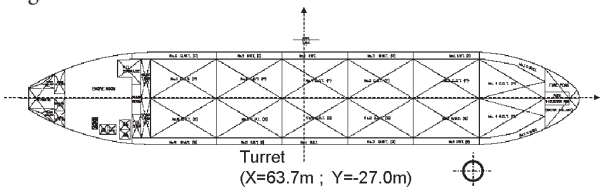

Fig. 4 Turret position considered in the simulations

A Jones Act hull, Chevron's Double Eagle - a 350,000 bbls tanker, was chosen as the ST (Figure 5).

The DP layout of both FPSO and ST are shown in Figure 6. The DP-FPSO is equipped with 6 CPP azimuthal thrusters, delivering 2.7MW per thruster, driven by a 4 x 6MW power generating system. The DP system[4] is required to keep the vessel position even after failure of two thrusters.

The DP-ST equipment meets station keeping performance with one 1.2MW Forward Azimuthal Thruster, one 0.75MW Aft Tunnel Thruster and one main CPP equipped with a high lift rudder (HLR). The ST is equipped for bow loading, with hawser and offloading hose. The ST is able to keep its own position, up to 33m/s (64 knots) wind speed, if weathervane, and up to 4m/s (8 Knots) wind speed, in a beam sea environment. For non-DP ST during offloading operations, a hold back tug force of 35tonf was considered.

Fig. 5 Up: FPSO MV Aberdeen (560,000 bbls). Down: Chevron's ST Double Eagle type (350,000 bbls).

4 DP3 + one generator or thruster out for maintenance.

Fig. 6 Above: DP-FPSO equipped with six azimuthal CPP thrusters. Turret shown at bow. Below: ST equipped with one Forward Azimuthal, one Aft Tunnel Thruster and one main CPP with a high lift rudder (HLR).

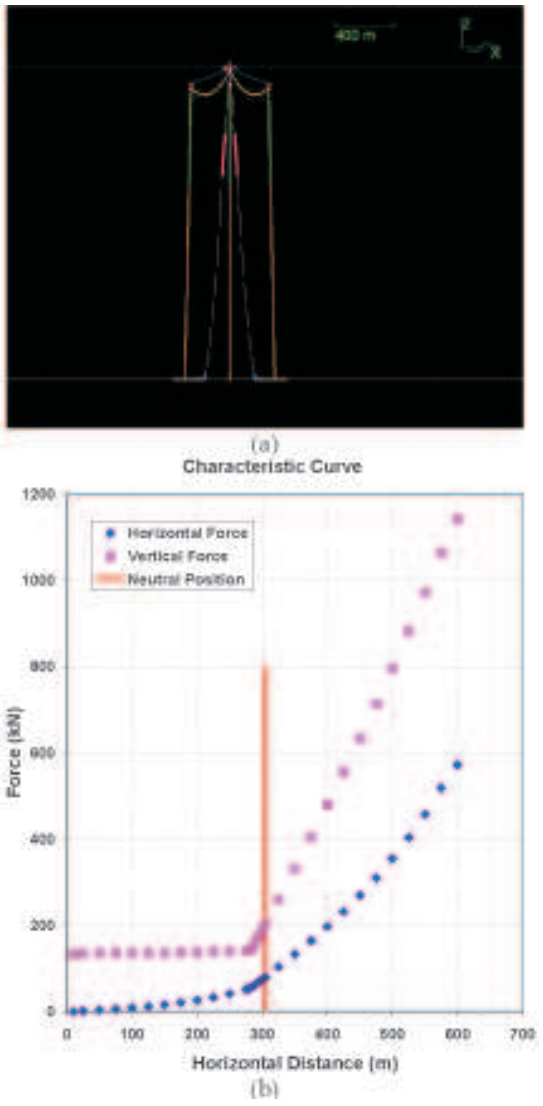

Fig. 7 (a) ORCAFLEX® Model and (b) Restoring force curve of one set (riser, buoy, tether and jumper)

The risers system with all its components (buoy, tether and jumper) was modeled using Orcaflex® (ORCINA, 2008) for evaluation of restoring characteristics and drag forces (Figure 7). A previous sensitivity analysis was carried out, in which the response

of DP-FPSO was compared for three - very distinct – values of mooring stiffness: the design (nominal) one; a very soft one, 5 times softer than the nominal one; a very rigid one, 5 times more rigid than the nominal one. DP-FPSO position-keeping and power demand were shown to be insensitive to such a huge variation on mooring stiffness, the difference of power consumption and positioning errors resulting smaller than 0.5%. For the sake of saving processing time, an equivalent line with the same restoring characteristic and equivalent drag was modeled instead of the real set (riser, buoy, tether and jumper).

Circa 380 full dynamic DP Simulations were run, aiming at investigating the behavior of the system: Riser + DP-FPSO+ ST (DP & non DP). The methodology adopted for the analysis and the main results will be discussed in the next sections.

3.1 DP capability plots and wind speed envelopes

DP capability analysis is generally used to establish the maximum weather conditions under which a DP vessel can keep its position and heading for a proposed thruster configuration. The environmental forces and moments are increased until they are statically balanced by the maximum available thrust offered by the thruster configuration. A limiting weather condition is therefore obtained as a combination of a given mean wind speed, significant wave height and sea current speed. Wind, current and waves are normally taken as coming from the same direction, (IMCA, 2000). By rotating the incidence of the environmental components with respect to the vessel, the results of a DP capability analysis may be presented by means of a limiting mean wind speed for a discrete number of wind angles of attack. The resulting polar plot is often referred to as a DP capability envelope. Usually, these plots are obtained through static equilibrium simulations. Instead, in the present work, the DP capability plots were constructed via dynamic simulations. Such an approach is much more complete and accurate, implying larger computational effort. The - wind speed envelopes - capability plots for both vessels (FPSO and ST), considering ballast and fully loaded conditions are presented in Figure 8. The relations between wave height and period with wind speed, shown in Figure 9, were obtained based on the Gulf of Mexico Metocean Data (GustoMSC, 2006). Current speed is here assumed to be constant, set to 0.3m/s.

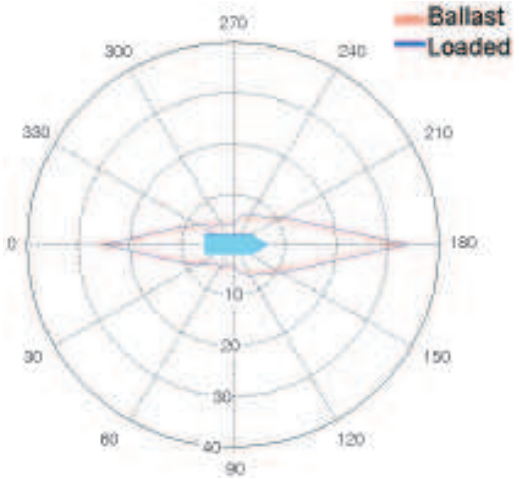

(a)

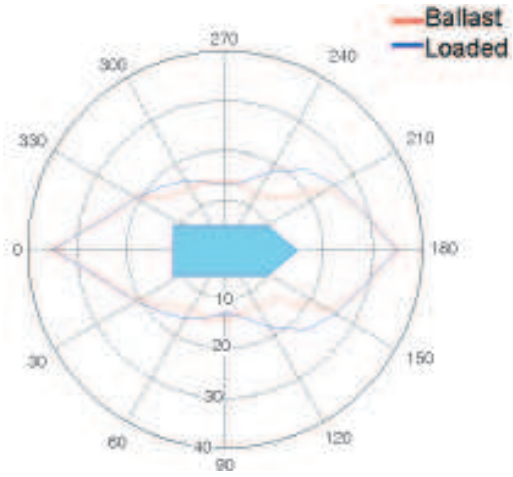

(b)

Fig. 8 Capability Plots: (a) ST; (b) FPSO. Wind speed in m/s.

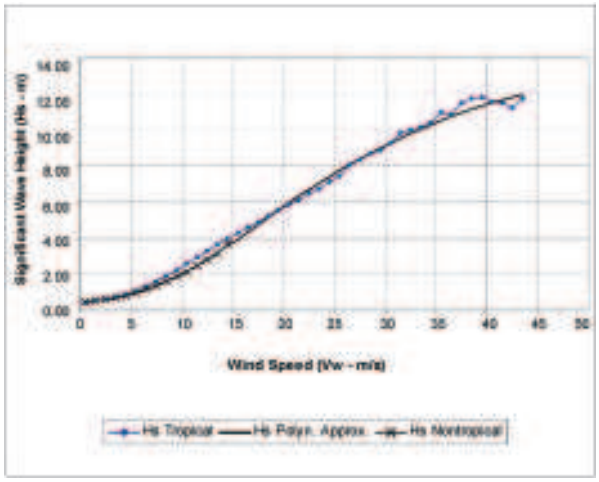

(a)

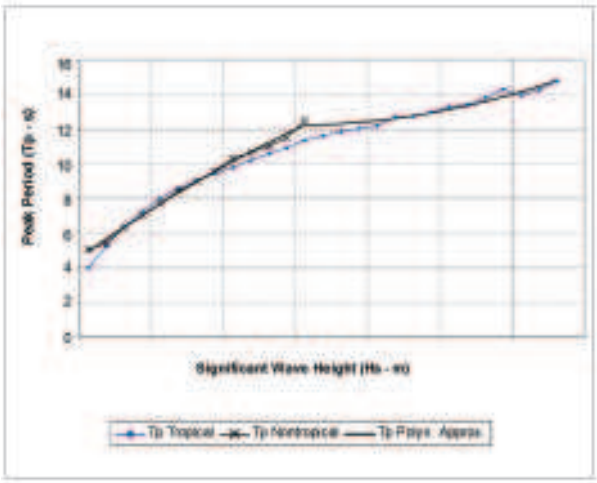

(b)

Fig. 9. Significant wave height (a) and peak period (b) with wind speed (non-tropical and tropical storms), including polynomial approximations.

3.2 Thrust and power utilization envelopes

Given a design sea-state, DP capability can be presented by means of thrust utilization envelopes instead of limiting wind speed envelopes. The required thrust to keep position and heading is then calculated and compared to the maximum available thrust. The ratio between them is plotted as a function of wind direction. A thrust or power utilization less than, or equal to 100% means the vessel is able to keep position and heading in the specified design sea state. If the ratio exceeds 100%, the vessel will experience poor positioning performance or will drift-off.

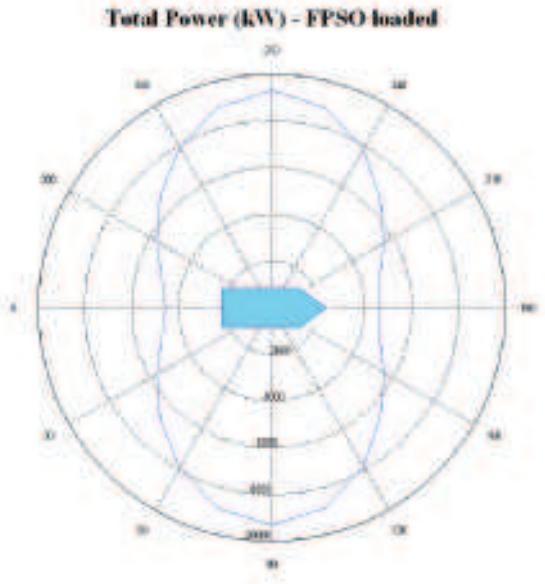

Fig. 10 Power utilization envelope for the loaded FPSO (alone) under 1.2 m/s (2.3knt) loop current - thrusters 1, 2, 3, 4 and 6 ON. Max power 9MW.

Power Utilization Envelopes were obtained for both, intact and thruster failure conditions. For example, considering all thrusters ON, the maximum delivered power is circa 9.5MW, (of a total of 10.8MW available power), as shown in Figure 10. In this illustrative case, the environmental condition is a 1.2m/s (2.3knots) loop current. Waves and wind are not considered.

3.3 Drifting-off and driving-off analysis

Two common failure modes were analyzed using the dynamic simulator. The first and important one is the drifting-off of the FPSO after a system blackout (a full power failure, turning all thrusters off). The simulation enables the designer to predict the time required to disconnect the turret. The maximum allowable offset for the disconnection defines the so-called "Survival Circle", in this case considered as a circle with a radius of 139m.

Figure 11 presents the drift of the ballasted FPSO after a blackout. Time series of the distance from the operational center point is presented for several wind speeds. It is also shown the full trajectory of the vessel considering a 10m/s wind condition.

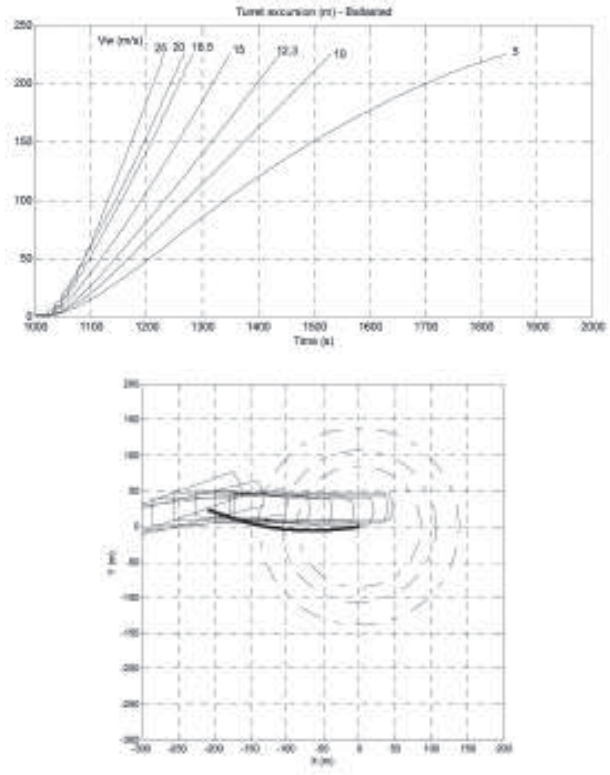

Fig. 11 (Up)Turret excursion after a blackout, occurred at t=1000.s (drift is measured from the operational center point); (Down) FPSO position tracking (wind speed 10m/s ; significant wave height 2.0m ; current speed 0.3m/s ; all environmental agents aligned).

A complete drifting-off analysis was carried out, and the main results are presented in Table 1. Drifting time is considered as being the time elapsed from the start of the blackout to the moment the turret point reaches the survival circle. The same wind-wave relation previously presented (Figure 9) is considered here. A 0.3m/s aligned current is also included. It can be seen that for wind speeds below 5m/s, the mooring system by itself is able to hold the ballasted FPSO within the desired limits. On the other hand, for a wind speed of 25m/s, the crew will have less than 3 minutes (166s) to the disconnection operation.

Table 1 **Drifting times (starting from operational center point)**

	Wind Speed		Load Condition	
	(m/s)	(knots)	Loaded	Ballast
Operating Point (center point) to Survival Circle	5.0	9.7	—(*)	462s
	10.0	19.4	490s	354s
	12.3	23.9	380s	300s
	15.0	29.2	288s	244s
	18.5	36.0	224s	200s
	20.0	38.9	210s	188s
	25.0	48.6	186s	166s

(*) in this case, mooring system by itself can hold the FPSO inside the Survival Circle.

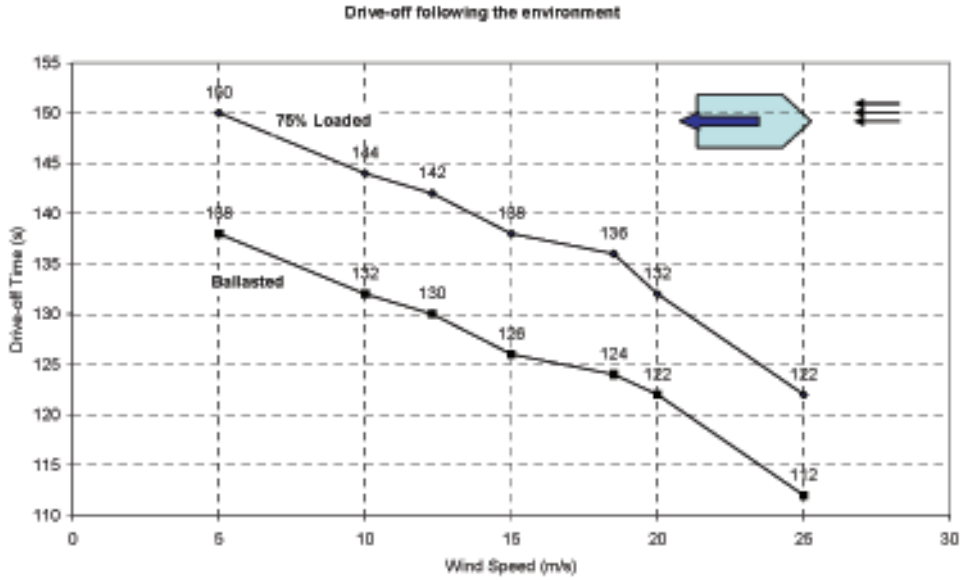

Fig. 12. Time to reach the Survival Circle after an astern drive-off failure. DP-FPSO alone.

Drive-off failures were also simulated. The term "drive-off" defines a failure in which the DP vessel is driven away from its target/desired position by its own thruster system, during a normal operation. Note that, in principle, drive-off might happen either ahead or astern leading to serious damage; particularly in the present case of a DP-FPSO. Obviously, this is an unplanned and very unwanted maneuver that would arise from serious logic failures. Main causes of a drive-off are: (i) failure of a local thruster control system; (ii) failure of DP system software and hardware; (c) failure of the positioning reference system or of other sensors. According to Chen and Moan (2004), who studied ST drive-off during offloading operation, this is a somewhat common DP failure. It is expected that 5.4 to 20 drive-off failures occur for every 1000 (tandem) offloading operations.

In the present work, dynamical simulations were used to evaluate the time required for disconnecting, after the very start of a drive-off failure. Both drive-off modes (ahead and astern) were simulated. The same environmental conditions used in the drifting-off analysis were considered.

Figure 12 presents the critical case: astern drive-off (following the environment). It can be seen that for the worst case (ballasted FPSO), the time to disconnection is lower than 112s.

3.4 Offloading operation

Two cases were considered for the DP-FPSO operation analysis: (i) offloading to a conventional ST (assisted by a tug boat, with a 35tonf bollard pull) and (ii) offloading to a DP-ST. The operational criteria for a safe operation comprehend: hawser tensioning and stretching limits; limitation of ST; relative distance between ST and FPSO. Each criterion is explained below.

1) Hawser limits of operation for a non-DP ST: the hawser system is a 200t SWL (safe working load) one, with 90m of overall length (10m chain+ 70m hawser cable + 10m chain). Operational limits considered are shown in Table 2.

Table 2 Operational limit criteria for the hawser system for a non-DP ST.

Hawser load trigger	Alarm/event	Action
70ton	High alarm activated	Alert
100ton	High-high alarm activated	Disconnect if more than 3 alarms in one hour
125ton	Emergency Shut Down (ESD)	Disconnect
Null(*)	High snapping load followed	Disconnect

2) Heading limitation for non-DP and DP STs: ideal operation is normally taken as to have the FPSO and ST directly aligned with each other. Table 3 shows the operating limit criteria applied in the present case.

Table 3 Operational limit criteria regarding ST heading envelope.

ST heading envelope (degrees w.r.t. to FPSO)	ST	Action
70	Non-DP	Pumping operation stopped (ESD)
80	Non-DP	ST disconnects and evades
80	DP	Pumping should be suspended
100	DP	ST disconnects and evades

3) Distance envelope for a DP shuttle tanker (hawser normally slack):
With the hawser normally slack, 70m is the target ST clearance aft the FPSO. A variation between 60m and 95m is admissible.

Table 4 Operational limit criteria regarding ST-FPSO clearance envelope.

ST clearance envelope (meters to FPSO)	Action
<60 or >95	Pumping operation stopped
<55 or >105	ST disconnects and evades

A brief illustration of all operational limits (for DP and non-DP ST) is presented in Figure 13.

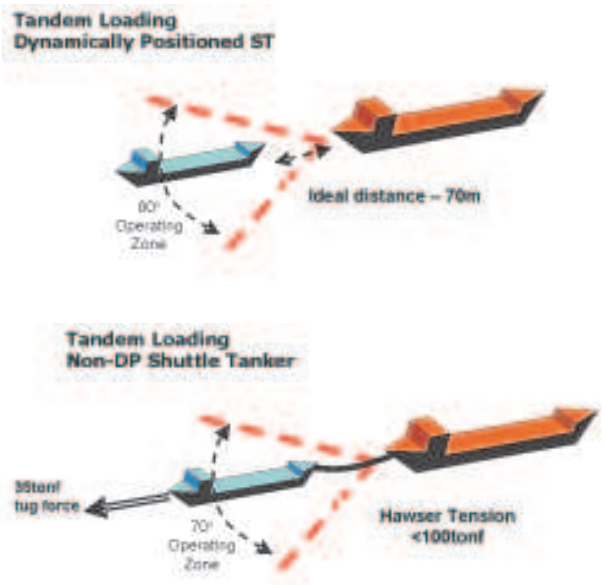

Fig. 13 DP-FPSO and non-DP ST: Operational limits

3.4.1 General Results

As one of the main results of the research, simulations indicated that the limit environmental condition is around 9 to 10m/s wind speed for the non-DP ST and 25 to 26m/s wind speed for the DP-ST. Table 5 shows limit wind speeds - under which all operational criteria are satisfied - obtained for two loading cases, as well as the corresponding operational criteria that would be violated if those limits were exceeded. Three conditions are exemplified with respect to the FPSO DP system integrity: no failure; one thruster; two thrusters. The limiting criterion for the non-DP ST is the maximum hawser tension (HT). This may explain why even under thruster failures the system may, in some cases, withstand slightly higher values of wind speed, as it becomes more compliant.

Table 5 Limit wind speeds and violating criteria.

Case\FPSO failure	No Failure	1 thruster fails	2 thrusters fail
Loaded DP-FPSO and ballasted non-DP ST	9.5 m/s (HT)	9.5m/s (HT)	10.5m/s (HT)
10% Cargo DP-FPSO and loaded non-DP ST	10.0 m/s (HT)	10.0m/s (HT)	10.0m/s (HT)
Loaded DP-FPSO and ballasted DP ST	25.5 m/s (C)	25.5 m/s (D)	25.5 m/s (D)
10% Cargo DP-FPSO and loaded DP ST	26.0 m/s (HT/C/HE)	26.0 m/s (HT/C/HE)	25.5 m/s (D)

In order to illustrate the comparison between non-DP and DP ST performances, the next sections present some simulation results regarding both offloading options, under critical environmental conditions.

3.4.2 Offloading from a DP-FPSO to a non-DP ST

The case of the non-DP ST during an offloading operation under 11m/s wind speed is illustrated in the following figures. FPSO thrusters 2 and 5 were supposed to fail. The FPSO is in loaded condition and the ST in ballast condition. Figure 14 presents the trace plot of both vessels during the whole simulation. Hawser tension, clearance and heading criteria are satisfied. The distance between the 90m length hawser connection points is also presented.

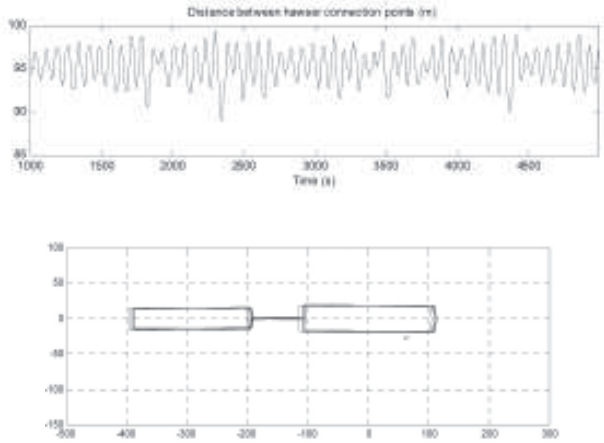

Fig. 14 FPSO and ST distance and tracing plot.

Figure 15 shows time series of turret position, FPSO heading angle and turret excursion. An XY plot of the turret position and a bar plot of the average power consumption of individual thrusters are also presented. Figure 16 shows time series of all DP-FPSO delivered thrust forces. Figure 17 presents the hawser tension time series. The tension reaches the high-high alarm value more than 3 times in one hour, and the operation is the considered as unsafe.

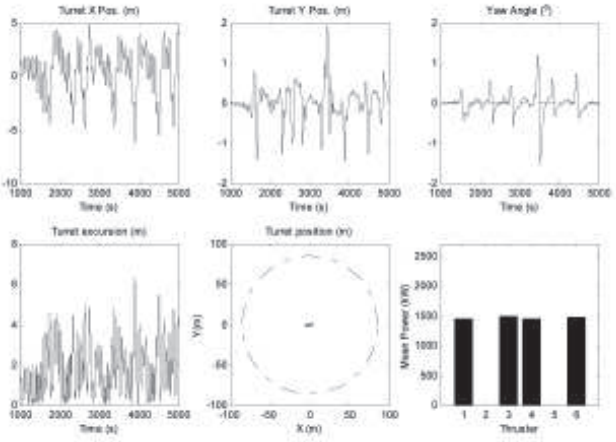

Fig. 15 Turret position, FPSO heading and delivered thrusters mean power.

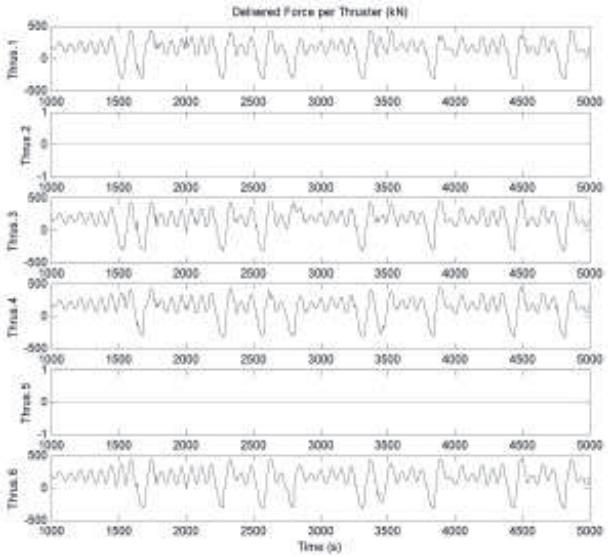

Fig. 16 Delivered thrusters forces: DP-FPSO.

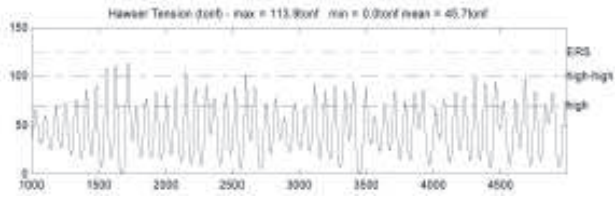

Fig. 17 Operational hawser tension limits reached, offloading from a DP-FPSO to a non DP ST.

3.4.3 Offloading from a DP-FPSO to a DP-ST

The case of a DP-ST, during an offloading operation under 25.5m/s wind speed, is now illustrated. As in the previous example, DP-FPSO thrusters 2 and 5 were supposed to fail. The FPSO is in loaded condition and the ST in ballast condition. Figure 18 presents the trace plot of both vessels, and the clearance between them. Hawser tension, clearance and heading criteria are satisfied. Both ships are aligned with each other and average clearance is approximately 70m.

A comparison between Figure 14 (non-DP ST) and Figure 18 (DP-ST) shows that the DP system installed in the ST reduces its longitudinal oscillations. Such oscillations are responsible for the dynamic load acting in the hawser (Figure 17) for the non-DP ST. This was the main limiting criteria for that operation (Table 5).

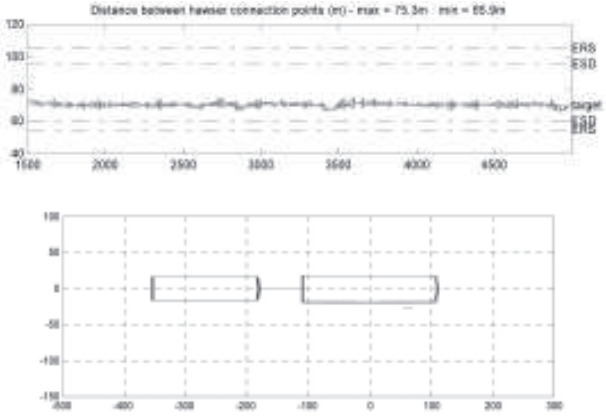

Fig. 18 FPSO and ST clearance and tracing plots.

Bar plots of the average power delivered by individual thrusters, for both DP-FPSO and DP-ST, are presented in Figure 19. At last, Figure 20 shows time series of thrust forces delivered by each ST thruster. In these figures, one may readily see that ST thruster number 1 is almost fully loaded. In fact, for a wind speed slightly higher than 25.5m/s the DP system loses position holding capacity, and ST will drift, in accordance to the results of Table 5.

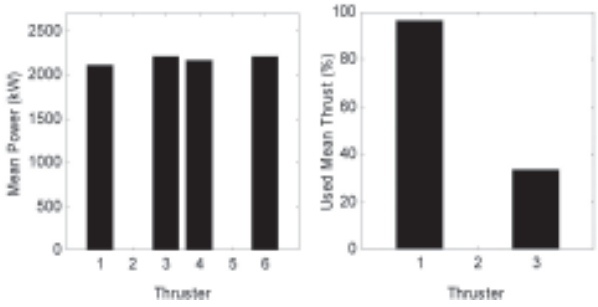

Fig. 19 Average power delivered by thrusters. Left: FPSO; right: ST.

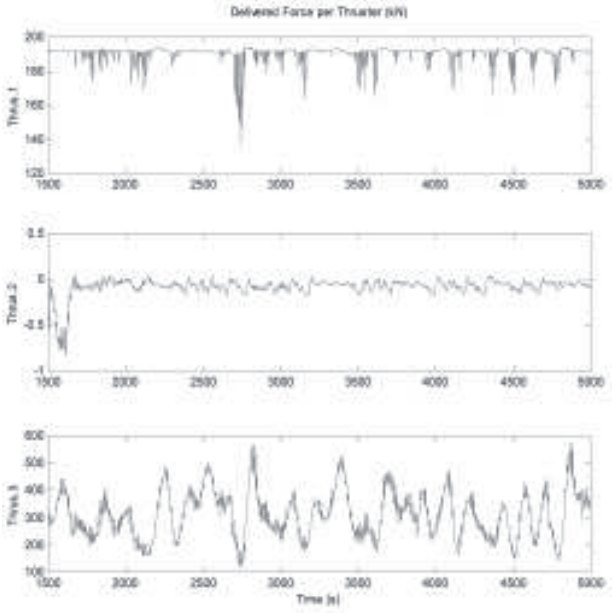

Fig. 20 Thrust forces delivered by each DP-FPSO thruster.

4 Conclusions

A thorough and comprehensive analysis program was planned and carried out by Chevron and other partners aiming at dimensioning DP and disconnection systems for a FPSO and a ST to operate in the Gulf of Mexico (GoM). This analysis encompassed: DP capability study; bow loading / side loading study; ship to ship transfer study; taut / slack hawser study; floating hose study; project look-back at similar conversions; Jones Act Tanker availability study. The paper presented a summary of the DP capability study achieved through an extensive program of full nonlinear dynamic simulations carried out at USP laboratories.

Important conclusions were derived from this study. The action of the DP system installed in the FPSO was shown to be insensitive to turret position and to the turret mooring stiffness. It was also shown that the DP-FPSO, alone, is able to keep its position in operational conditions, even with 2 thrusters down.

Simulations indicated that FPSO emergency disconnection should be performed in less than 2 minutes in the case of a drive-off and 3 min in case of a drift-off failure, therefore requiring prompt action and an efficient emergency procedure. When offloading to a ST, the limit values of wind speeds are much higher for the DP-ST case (up to 25 m/s) than those for the non-DP ST case (up to 9m/s). The main violating criterion for the non-DP ST was found to be hawser tension. On the other hand, it was also shown that the DP system installed in the ST reduces its longitudinal oscillations, responsible for the dynamic load acting in the hawser for the non-DP ST case, therefore hawser tension to exceed allowable values. For the DP-ST, the limiting weather condition is defined by the DP holding capacity, i.e., ability to keep the ST inside the safe zone defined for the offloading operation.

As main conclusions, the present study pointed out that DP-systems do give the highest berthing assurance, precluding hold-back tug. The outcome of the analysis discussed in this paper was used as input for evaluating the downtime of the FPSO-ST system, in both DP and non-DP ST configuration. Results indicate that the FPSO-ST system can operate safely, on station, with a projected down-time of circa 4%. On the other hand, the non-DP ST down-time was predicted to be beyond 14%. It is expected that loop currents might increase this figure a little (Ferreira and Howard, 2007). Comprehensive risk and reliability analysis are still to be completed.

5 Acknowledgments

The authors thank Chevron, for supporting this research study. Special acknowledgments go to Petrobras, CNPq and FAPESP, for giving USP team a continuous support on FPSO and DP research, during these last ten years.

6 References

Aranha, J.A.P., "A Formula for Wave Damping in the Drift of a Floating Body", Journal of Fluid Mechanics, vol. 272, pp.147-155, 1994.

Aranha, J.A.P., Martins M.R., "Low frequency wave force spectrum influenced by wave-current interaction", Applied Ocean Research 23(3), pp. 147-157, 2001.

Aranha, J.A.P., da Silva S., Martins M.R., Leite A.J.P, "A weathervane ship under wave and current action: an experimental verification of the wave drift damping formula", 23(1) pp. 103-110, 2001.

Balchen, J.G., Jenssen, N.A., Mathisen, E., Saelid, A., Dynamic positioning system based on Kalman filtering and optimal control, Modeling, Identification and Control, Vol. 1, No. 3, 1980, pp. 135-163.

Bravin, T.T., Tannuri, E.A, "Dynamic Positioning Systems Applied to Offloading Operations", International Journal of Maritime Engineering (IJME), vol. 146, Part A2, 2004.

Chen, H., Moan, T., "Probabilistic modelling and evaluation of collision between shuttle tanker and FPSO in tandem offloading", Reliability Engineering and System Safety 84 (2004) 169-186, 2004.

DNV, Det Norsk Veritas, Rules of Classification of Mobile Offshore Unities, Part 6, Chapter 7, July, 1989.

Ferreira, P.R., Howard, N., DP FPSO for GoM Considerations for the FPSO and Shuttle Tanker, FPSO Forum, Houston, 2007.

FOSSEN, T. I., Guidance and Control of Ocean Vehicles, John Wiley and Sons Ltd., West Sussex, England, 1994.

GUSTOMSC, "Project DP FPSO - Dynamic Positioning Capability Report", (provided by Chevron), 2006.

IMCA, The International Maritime Contractors Association, Specification for DP Capability Plots, IMCA M140 Rev. 1, 2000.

NISHIMOTO, K., Kaster, F., Masetti, I.Q., Matsuura, J., Aranha, J.A.P., "Full Scale Decay Test of a Tanker: Field Data and Theoretical Analysis". Ocean Engineering, United Kingdom, V. 26, N. 2, P. 125-145, 1999.

OCIMF, "Predictions of wind and current loads on VLCCs", Oil Companies International Marine Forum, 1994.

ORCINA, "ORCAFLEX Manual Version 9.1a", Orcina Ltd, 2008.

SIMOS, A.N., Pesce, C.P., Tannuri, E.A., Aranha, J.A.P., "Quasi-explicit Hydrodynamic Model for the Dynamic Analysis of a Moored FPSO Under Current Action", Journal of Ship Research, 45(4), 289-301, 2001.

SØRDALEN, O.J., "Optimal Thrust Allocation for Marine Vessels", Control Engineering Practice, Vol.5, No.9, pp. 1223-1231, 1997.

TANNURI, E.A., "Desenvolvimento de Metodologia de Projeto de Sistema de Posicionamento Dinâmico Aplicado a Operações em Alto-Mar", PhD Thesis, (In Portuguese), University of São Paulo, supervisor: C. P. Pesce, 2002 (http://www.teses.usp.br/teses/disponiveis/3/3132/tde-04082003-173204/).

TANNURI, E.A., Donha, D.C., Pesce, C.P., "Dynamic Positioning of a Turret Moored FPSO Using Sliding Mode Control", International Journal of Robust and Nonlinear Control, Vol. 11, pp. 1239-1256, 2001.

TANNURI, E.A., Kubota, L, Pesce, C.P., "Adaptive Control Strategy for the Dynamic Position of a Shuttle Tanker during Offloading Operations", Journal of Offshore Mechanics and Arctic Engineering, Vol. 128, pp. 203-210, 2006.

TANNURI, E.A., Leite, A.J.P., Simos, A.N., Aranha, J.A.P., "Experimental validation of a Quasi-explicit Hydrodynamic Model: fishtailing instability of a single-point moored tanker in rigid-hawser configuration", Journal of Ship Research, 45(4), pp 302-314, 2001.

WAMIT, "WAMIT User Manual Versions 6.0, 6.0PC, 5.3S", WAMIT Inc., MA, USA, 2000.

Appendix - DP system algorithms

This appendix presents a full description of the algorithms used in the simulation code for modeling the DP System response.

EXTENDED KALMAN FILTER (EKF)

With X_L and Y_L being the position of the central point of the vessel, ψ_L the heading angle, the low frequency motion can be described by:

$$\dot{\mathbf{x}}_L = \mathbf{A}_L^{6\times6}\mathbf{x}_L + \mathbf{A}_{EL}^{6\times3}\mathbf{F}_E + \mathbf{E}_L^{6\times3}\boldsymbol{\omega}_L + \mathbf{B}_L^{6\times3}\mathbf{F}_T \qquad (1)$$

where

$$\mathbf{A}_L^{6\times6} = \begin{pmatrix} \mathbf{0}_{3x3} & \mathbf{T}(\psi_L) \\ \mathbf{0}_{3x3} & -\mathbf{M}^{-1}\mathbf{C}_{3x3} \end{pmatrix};\ \mathbf{A}_{EL}^{6\times3} = \mathbf{B}_L^{6\times3} = \mathbf{E}_L^{6\times3} = \begin{pmatrix} \mathbf{0}_{3x3} \\ \mathbf{M}^{-1} \end{pmatrix}$$

$\mathbf{x}_L = \begin{pmatrix} X_L & Y_L & \psi_L & \dot{x}_1 & \dot{x}_2 & \dot{x}_6 \end{pmatrix}^T$, F_T are thruster forces and moment vector, F_E are low frequency external forces and moment vector (including environmental and mooring forces). $\boldsymbol{\omega}_L$ is a 3x1 vector containing zero-mean Gaussian white noise processes with covariance matrix $\mathbf{Q}_L$ ($\boldsymbol{\omega}_L \sim N(0,\mathbf{Q}_L)$). The subscript L is related to low frequency motion. **M** is the mass matrix and C is a damping matrix of the system, respectively given by:

$$\mathbf{M} = \begin{pmatrix} M+M_{11} & 0 & 0 \\ 0 & M+M_{22} & M_{26} \\ 0 & M_{26} & I_Z+M_{66} \end{pmatrix} \qquad (2)$$

$$\mathbf{C} = \begin{pmatrix} C_{11} & 0 & 0 \\ 0 & C_{22} & 0 \\ 0 & 0 & C_{66} \end{pmatrix}$$

The forces F_E are modeled as slowly-varying unknown parameters. A mathematical model of such variables may be expressed as:

$$\dot{\mathbf{F}}_E = \boldsymbol{\omega}_{FL} \qquad (3)$$

where $\boldsymbol{\omega}_{FL}$ is a 3x1 vector containing zero-mean Gaussian white noise processes with covariance matrix $\mathbf{Q}_{FL}$ ($\omega_{FL} \sim N(0,\mathbf{Q}_{FL})$). In other words, it is assumed that the time-derivative of the environmental forces are small, representing the fact that they are slowly-varying.

Finally, high-frequency horizontal motions of the vessel may be approximated by a linear model. Such model fits the shape of wave-induced motion spectrum. It was described by Balchen et al., 1980 and Fossen, 1994, and is given by:

$$\begin{aligned} \dot{\mathbf{x}} &= \mathbf{A}(\mathbf{x})\mathbf{x} + \mathbf{B}\mathbf{F}_T + \mathbf{E}\boldsymbol{\omega} \\ \mathbf{z} &= \mathbf{H}\mathbf{x} + \mathbf{v} \end{aligned} \qquad (4)$$

with **x**, **ω**, **A(x)**, **B**, **E** and **H** according to Equations (1), (3), (4) and (5).

where is a 3x1 vector containing zero-mean Gaussian white noise processes and the subscript H represents high frequency. The parameter is a damping coefficient ratio, introduced in the model in order to better fit the Pierson-Moskowitz spectrum, and was set as 0.1. The parameter ζ represents the high frequency (wave-induced) motions peak frequency.

The measured signals **z** are given by:

$$\mathbf{z} = \begin{pmatrix} X_L + X_H + v_X \\ Y_L + Y_H + v_Y \\ \psi_L + \psi_H + v_\psi \end{pmatrix} \tag{5}$$

where $\mathbf{v} = \begin{bmatrix} v_X & v_Y & v_\psi \end{bmatrix}^T$ is a 3x1 vector containing zero-mean, Gaussian white noise processes (**v**~N(0,**R**)).

For the sake of simplicity, the matrixes Q_L, Q_H, Q_{FL} and R are considered diagonal in real applications. It should be emphasized that the EKF (Extended Kalman Filter) estimates the components x_H and x_L as well as the low frequency environmental forces F_E.

The complete model can be written as:

$$\begin{aligned} \dot{\mathbf{x}} &= \mathbf{A(x)x} + \mathbf{BF_T} + \mathbf{E\omega} \\ \mathbf{z} &= \mathbf{Hx} + \mathbf{v} \end{aligned} \tag{6}$$

with **x, ω, A(x), B, E** and **H** according to Equations (1), (3), (4) and (5).

The following discrete version of Equation (6) is used in the EKF algorithm, being t the sampling time:

$$\begin{aligned} &\mathbf{x}[k] = \mathbf{f}(\mathbf{x}[k-1], \mathbf{F}_T[k-1], \boldsymbol{\omega}[k-1]) \\ &\mathbf{z}[k] = \mathbf{H}.\mathbf{x}[k] + \mathbf{v}[k] \\ &\mathbf{f}(.,.,.) = (\mathbf{A(x)}.\Delta t + \mathbf{I}).\mathbf{x}[k-1] + \mathbf{B}.\Delta t.\mathbf{F}_T[k-1] + \mathbf{E}.\Delta t.\boldsymbol{\omega}[k-1] \end{aligned} \tag{7}$$

With the model written in the discrete version (7), a discrete EKF algorithm can be directly applied. Defining $\bar{\mathbf{x}}$ as an *a priori* estimate, $\hat{\mathbf{x}}$ as an *a posteriori* estimate of state vector, respectively, the a priori $\bar{\mathbf{X}}$ and $\hat{\mathbf{X}}$ a posteriori estimates of error matrix covariance, and K the Kalman gain matrix, the discrete EKF is given by:

$$\begin{aligned} &\bar{\mathbf{x}}[k+1] = \mathbf{f}(\hat{\mathbf{x}}[k], \mathbf{F}_T[k], 0) \\ &\bar{\mathbf{X}}[k+1] = \boldsymbol{\Phi}.\hat{\mathbf{X}}[k].\boldsymbol{\Phi}^T + \boldsymbol{\Gamma}.\mathbf{Q}.\boldsymbol{\Gamma}^T \end{aligned} \quad \text{(Predictor)} \tag{8}$$

with

$$\boldsymbol{\Phi} = \partial \mathbf{f} / \partial \mathbf{x}\big|_{\mathbf{x}=\hat{\mathbf{x}}[k]}; \boldsymbol{\Gamma} = \mathbf{E}.\Delta t; \quad \mathbf{Q} = diag\begin{pmatrix} \mathbf{Q}_L & \mathbf{Q}_H & \mathbf{Q}_{FL} \end{pmatrix}$$

$$\begin{aligned} &\mathbf{K}[k] = \bar{\mathbf{X}}[k].\mathbf{H}^T.\left(\mathbf{H}.\bar{\mathbf{X}}[k].\mathbf{H}^T + \mathbf{R}\right)^{-1} \\ &\hat{\mathbf{x}}[k] = \bar{\mathbf{x}}[k] + \mathbf{K}[k].\varepsilon[k] \\ &\hat{\mathbf{X}}[k] = \left(I - \mathbf{K}[k].\mathbf{H}\right).\bar{\mathbf{X}}[k] \end{aligned} \quad \text{(Corrector)} \tag{9}$$

where $\varepsilon[k] = \left(\mathbf{z}[k] - \mathbf{H}.\bar{\mathbf{x}}[k]\right)$ is the innovation term.

CONTROLLER

The controller most widely used in DP systems:

There is a feed-forward wind force compensator, which utilizes the wind speed and direction measured by an anemometer and a simplified model for the estimation of the forces acting on the vessel. Such forces are directly compensated by the controller, and they are counteracted before causing a positioning error.

A Proportional-Derivative (PD) feedback controller compares the desired set-points with the estimated positions and heading, $\hat{\mathbf{x}}_L$, and calculates the forces to minimize such a difference

Finally, the integral action is given by the subtraction of the low frequency environmental forces $\hat{\mathbf{F}}_E$ that are estimated by the EKF.

Figure 21 presents a block diagram of the EKF and the controller.

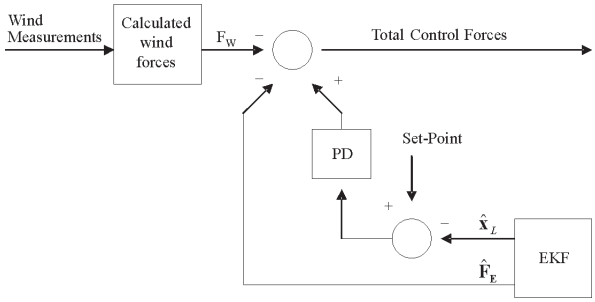

Fig. 21. EKF and controller block diagram

PD control gains are adjusted by standard pole-placement techniques, based on a linear model obtained from Equation (6) for each direction, namely surge, sway and yaw, assuming they are uncoupled.

THRUST ALLOCATION

The thrust allocation logic is responsible for delivering moment and forces calculated by control module algorithms. Such algorithms are oriented towards fuel consumption minimization. The implemented technique, described by Sørdalen (1997), is based on a pseudo-matrix inversion, and minimizes the quadratic summation of delivered thrusts. The resultant thrust vector T is given by:

$$\mathbf{T} = (\mathbf{A}^T\mathbf{A})^{-1}\mathbf{A}^T\mathbf{F_T} \tag{10}$$

where, $F_T = (F_{1T}, F_{2T}, F_{6T})^T$ represents the demanded control forces and moment, and:

$$\mathbf{A} = \begin{pmatrix} 1 & . & 1 & 0 & . & 0 & c_{1+n_{azim}} & . & c_{n_{prop}} \\ 0 & . & 0 & 1 & . & 1 & s_{1+n_{azim}} & . & s_{n_{prop}} \\ -x_{2,1P} & . & -x_{2,n_{azim}P} & x_{1,1P} & . & x_{1,n_{azim}P} & -c_{1+n_{azim}}.x_{2,(1+n_{azim})P} + s_{1+n_{azim}}.x_{1,(1+n_{azim})P} & . & -c_{n_{prop}}.x_{2,n_{prop}P} + s_{n_{prop}}.x_{1,n_{prop}P} \end{pmatrix} \quad (11)$$

being $c_i = \cos(\alpha_{iP})$ e $s_i = \sin(\alpha_{iP})$ where α_{iP} is the azimuth angle when using azimuthal propellers and xi gives the position of the propeller, according to an orthogonal reference frame fixed to the vessel. The vector **T** contains surge and sway force components required in each available propeller, fixed or azimuthing. The required azimuth and thrust are directly obtained from such components.

Some extra features are also included in the allocation algorithm, as follows:

- Reallocation of demanded forces and moment: if the nominal power of a propeller is occasionally exceeded, the difference between the total forces and moment required by the controller and those delivered by the propeller system is calculated, and the difference is reallocated among the non-saturated propellers;
- Dead zone control: defines prohibited azimuth angles for each propeller, in order to minimize the interference between two propellers or between a propeller and the hull.
- Control of rotation reversal: some propellers are not able to reverse the rotation of their blades or may present a reduced efficiency under reversed rotation. Therefore, the allocation algorithm defines a maximum time interval, within which the rotation can remain reversed until the azimuth angle is rotated by 180o and the propeller rotation re-established.
- Azimuth filter: it consists of an important way to minimize azimuth oscillation caused by fluctuation of small required control forces. The implemented filter was a classic first order low-pass one, designed to attenuate frequencies higher than 0.1Hz.